Urban Climate xxx (xxxx) 101608

Contents lists available at ScienceDirect

Urban Climate

journal homepage: www.elsevier.com/locate/uclim

Quantification of primary $PM_{2.5}$ Mass Exchange in three Mexican Megalopolis Metropolitan Areas

Adolfo Hernández-Moreno, Fátima I. Trujillo-Páez, Violeta Mugica-Álvarez *

Basic Sciences Department, Universidad Autónoma Metropolitana, Unidad Azcapotzalco. Av. San Pablo No. 420, Col. Nueva el Rosario, Azcapotzalco C.P., 02128 Ciudad de México, México.

ARTICLE INFO

Keywords:
Hysplit
$PM_{2.5}$
Mexico City megalopolis
Toluca
Cuernavaca
Mass exchange

ABSTRACT

It is commonly assumed that the outgoing flux of pollutants from large cities deteriorates the air quality of neighboring communities. Quantifying the mass exchange of pollutants among cities will enable local and regional planning of environmental management programs, to identify well all previously unrecognized impacted areas. In this study, the quantification of outgoing and incoming fluxes of primary $PM_{2.5}$ particle mass among three neighboring metropolitan areas of the Mexico City Megalopolis in the dry-cold climate months, was carried out for the first time. The results show that the metropolitan areas of Toluca Valley and Cuernavaca receive mass quantities of $PM_{2.5}$ approximately equivalent to a 100% of their local emissions. The prevailing winds in the cold-dry climate months, impel the emissions from the studied metropolitan areas, effectually dispersing in different directions, though mainly towards the megalopolis South, impacting with large mass amounts of $PM_{2.5}$ the rural areas. The overlap puffs of local emissions with imported particle masses contribute to atypically high concentration events in receiving metropolitan areas. In the import-export balance, the metropolitan areas of Toluca and Cuernavaca had a significant $PM_{2.5}$ concentration increasing during the cold-dry climate months mainly due to the incoming particles from the Mexico City Metropolitan Area.

1. Introduction

The pollutants released into the atmosphere are most certainly transported across different political borders. Hence, generating entities become air pollutants sources and, therefore, convey their negative impacts on the environment and human health, bringing about such maladies as respiratory diseases and premature mortality, (Balakrishnan et al., 2015; Hoek et al., 2013; IARC, 2016). For this reason, air quality management must be accomplished with a multi-scale vision: local, regional, and global, considering the pollutant half-life in the atmosphere. Pollutant emissions from urban zones impact negatively the surrounding areas so, rural and sparsely urbanized areas would suffer, most likely, the effects of air pollution from a large neighboring city. Likewise, the air pollution in an urban area can be aggravated due to greater quantities of pollutants brought in from the neighboring sources (Chacón et al., 2021; Dedoussi et al., 2020; Emmons et al., 2010; Sergi et al., 2020). The impact of the air pollutant incoming flux will depend on the ventilation allottable as a result of flow dynamic hindrances proper of mountain elevations. Effectually, the orography can cause the formation of atmospheric basins where the climate and meteorology have a typical behavior at the region (Magaña and Caetano,

* Corresponding autor.
E-mail address: vma@azc.uam.mx (V. Mugica-Álvarez).

https://doi.org/10.1016/j.uclim.2023.101608
Received 25 December 2022; Received in revised form 1 June 2023; Accepted 8 July 2023
2212-0955/

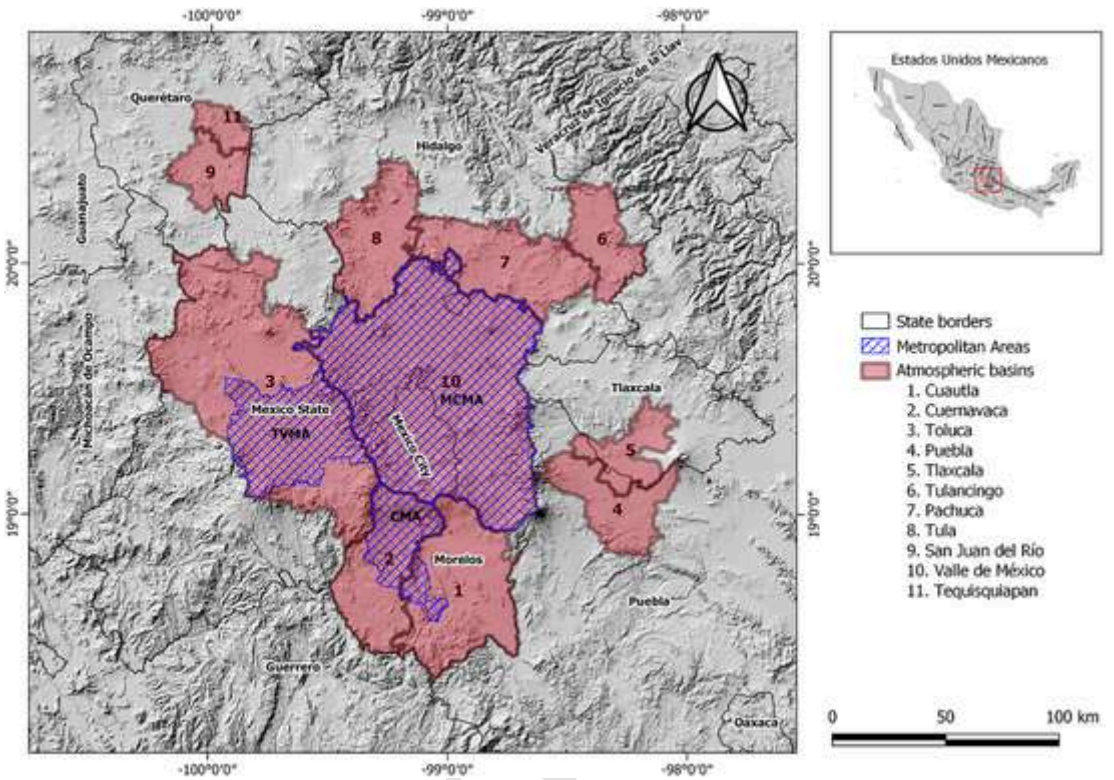

Fig. 1. Study area including the metropolitan areas of Mexico City, Toluca Valley and Cuernavaca.

Table 1
Emissions of $PM_{2.5}$ by metropolitan area.

Pollutant	TVMA	MCMA	CMA
PM2.5 [kg hour $^{-1}$]	203.8	860.6	114.2

2007). The formation of an atmospheric basin implies a greater retention of pollutants as well as greater recirculation and suspension of these, conversely to orographically open regions.

When the terrain characteristics promote the formation of contiguous atmospheric basins with intense urban activity, a particular situation rises which, more likely than not, would worsen, because pollutants addition to an already widely-polluted basin augments its function-of-time concentration, virtually distancing remedial plans. In this case, the pollutants incoming from one basin, are capable of interacting readily in their new basin-atmosphere such that active mass transport modes begin to operate actively, thus facilitating the levelling off of the concentration gradients in large atmospheric masses; therefore, the impact intensity in these scenarios is more relevant because the brought in pollutants must now be added to the native air pollutants emitted in the receptor basin, resulting in further air quality deterioration and increasing proportion of associated premature mortality (Dedoussi et al., 2020). Many air flow studies among atmospheric basins have published analyzed monitoring data and meteorological models, such as MM5 (De Foy et al., 2006, 2008; Jazcilevich et al., 2003; Magaña and Caetano, 2007). The wind patterns shed light on the formation of atmospheric basins and the identification of orographic channels through which the incoming and outgoing flows of air masses are more frequent. However, knowledge of flow patterns is insufficient to measure the exchange of pollutants impacts. The mass of incoming pollutants could deteriorate the air quality of the receiving basin to levels that local emissions would not cause. Winds that should naturally aerate a basin could introduce polluting masses and counteract the local outgoing pollutant emissions.

The Mexico City Megalopolis (MCM) includes 224 municipalities in the states: Hidalgo, Mexico, Morelos, Puebla and Tlaxcala, in addition to the 16 municipalities of Mexico City (DOF, 2013). Some of the MCM municipalities are grouped into highly urbanized and industrialized metropolitan areas, such as the Mexico City Metropolitan Area (MCMA), Toluca Valley Metropolitan Area (TVMA) and Cuernavaca Metropolitan Area (CMA). The definition of the MCM intersects with eleven atmospheric basins, which exchange pollutants in seasonal regimes, particularly through certain orographic channels (CAMe, 2018; Magaña and Caetano, 2007; SMAEM, 2007).

The Hysplit hybrid model, that is capable of establishing source-receptor relationships over long distances, has been used in a large number of studies around the world (Bera et al., 2022; Huang et al., 2020; Molina et al., 2019; Yerramilli et al., 2012), whereas its application in Mexico includes pattern identification and concentration estimations through forward and backward trajectory

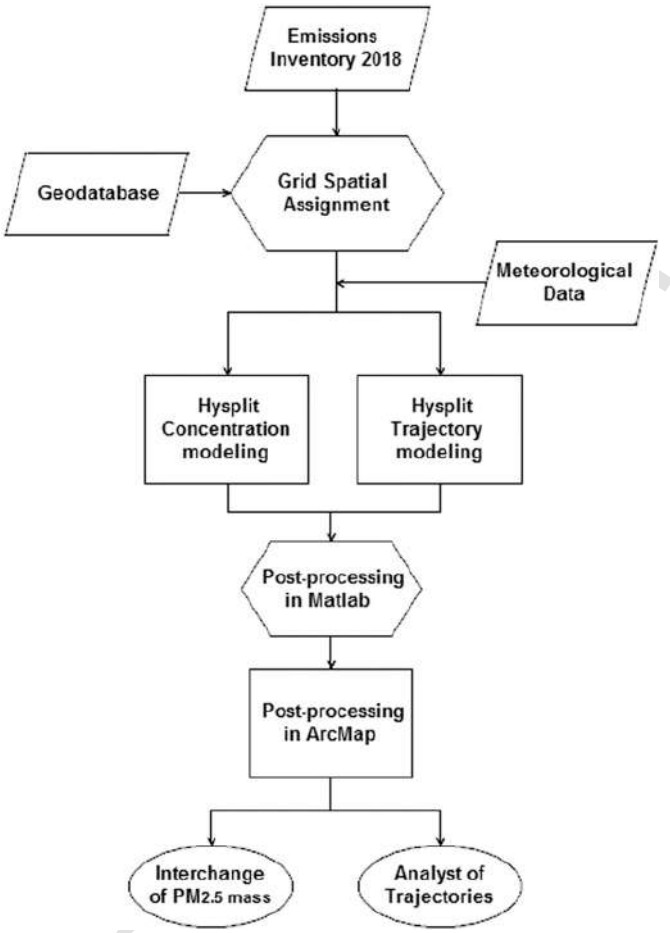

Fig. 2. Flow diagram for the mass exchange quantification among metropolitan areas and statistical analysis of transport trajectories.

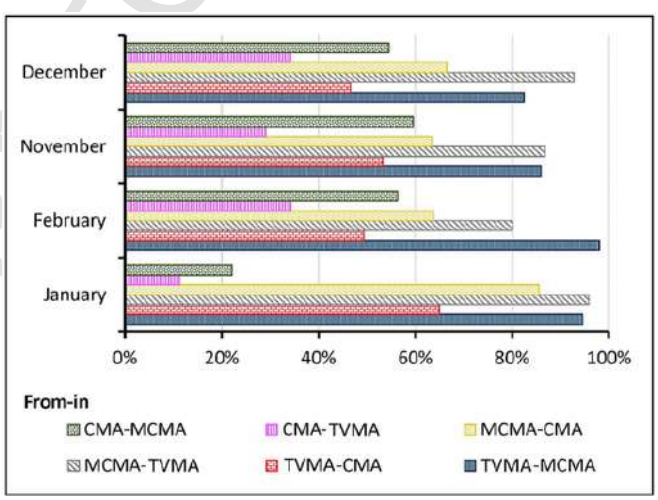

Fig. 3. Percent of hours when particles from one metropolitan area were located in another metropolitan area in the dry-cold climate months.

modeling (Flores-Ortiz et al., 2021; Sisneros, 2014; Tzompa-Sosa et al., 2016), PM_{10}, $PM_{2.5}$ and pollen transport modeling (González-Cardoso et al., 2020; González et al., 1999), as well as emission dispersion models from fixed sources (González-Cardoso et al., 2020; Ortinez-Alvarez et al., 2021). Nevertheless, as stated before, the knowledge of air flow patterns and estimated concentrations among atmospheric basins are not enough to evaluate the impact related to the pollutants exchange on the air quality of the metropolitan ar-

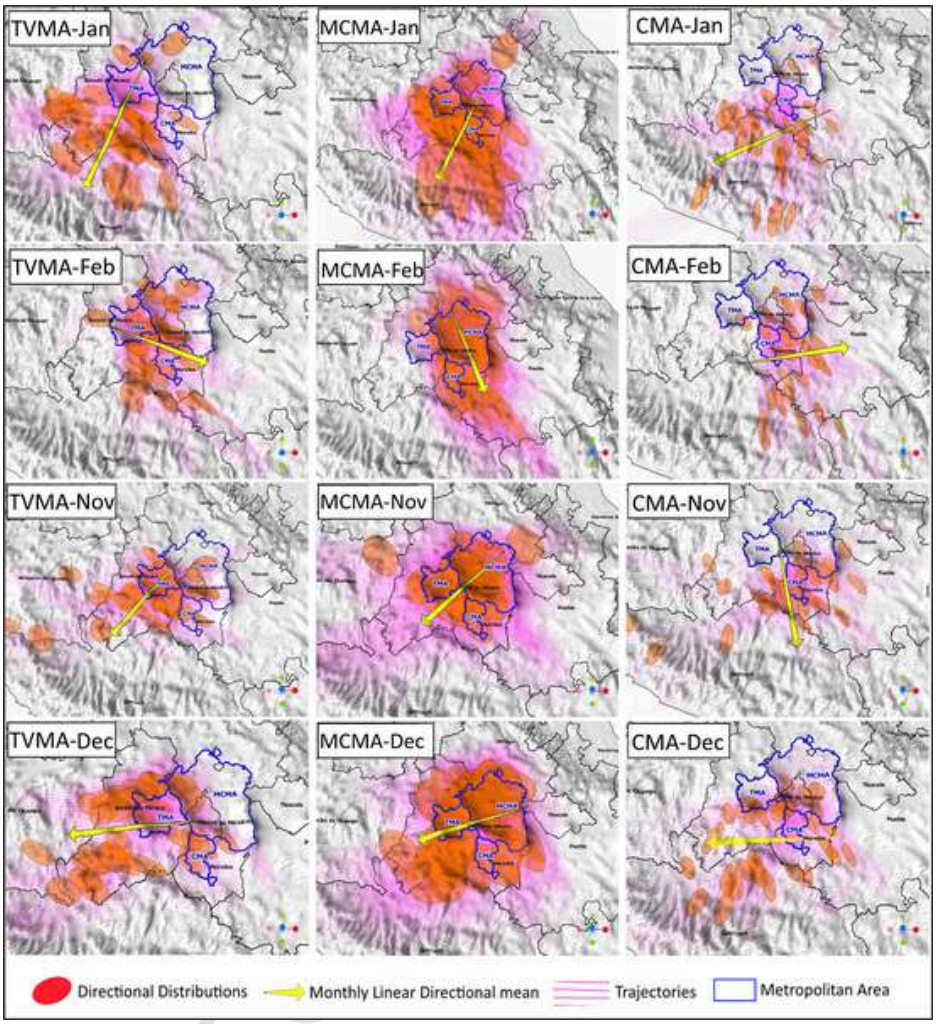

Fig. 4. Analysis of impact patterns of dispersion trajectories. Directional distribution identifies the areas mostly impacted by $PM_{2.5}$ emissions from each metropolitan area. The monthly linear directional mean is a summary of the directional trend in 2018.

eas into the receiving basin since the incoming pollutant mass could counteract the emission control measures from instituted local management programs and increase the pollution levels in already highly polluted urban areas. To estimate the impact of pollutants mass exchange among metropolitan areas, the dispersion of primary $PM_{2.5}$ emissions from three adjacent metropolitan areas was modeled, and the incoming and outgoing masses of each zone during the cold-dry season were quantified for the first time.

2. Methodology

The study area included the Toluca Valley Metropolitan Area (TVMA), the Cuernavaca Metropolitan Area (CMA), and the Mexico City Metropolitan Area (MCMA), in the central region of Mexico (Fig. 1). Toluca Valley and Cuernavaca Metropolitan Areas share a border with the MCMA, while Toluca and Cuernavaca are separated by the Neovolcanic mountain range.

The point and area source emissions were taken from the Megalopolis Emission Inventory of 2018 provided for the Environmental and Natural Resources Ministry (SEMARNAT, by its Spanish acronym) (SEMARNAT, 2016, 2022).

The Hysplit model can turn off emission sources when computational capabilities are exceeded by attempting to model the dispersion of millions of particles simultaneously. In modeling works, frequently emissions are aggregated in cells of a grid (Badia et al., 2023; García-R et al., 2000; Tran et al., 2023), allowing reduction of thousands of emission source coordinates to a few hundred, and making the modeling work possible, which otherwise would not be in a disaggregated way. Additionally, including the emissions in cells allow the personal information protection as is required by the Mexican Federal Law on Protection of Personal Data Held by Private Parties; then, for this study, the emissions were added to a grid with 5 × 5 km cells. Dispersion and trajectories were modeled in hourly intervals. Table 1 summarizes the hourly emissions modeled by each metropolitan area. The emissions of each metropolitan area were spatially distributed in a mesh with cells of 5 × 5 kilometers. Dispersion and trajectories were modeled in hourly intervals. Table 1 summarizes the hourly emissions modeled by each metropolitan area.

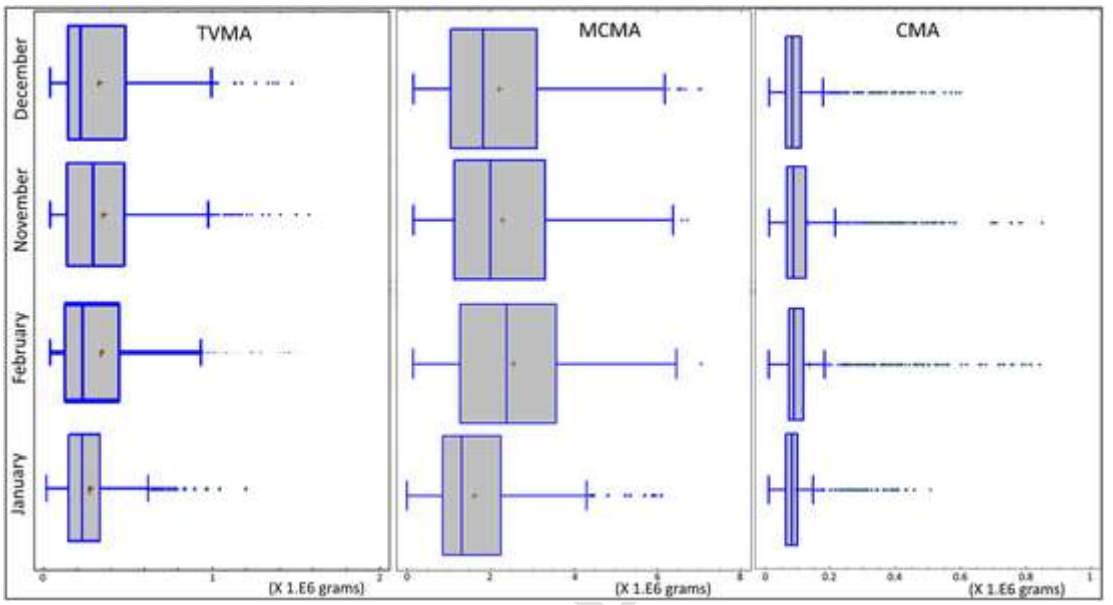

Fig. 5. $PM_{2.5}$ mass daily retention in the cold-dry climate months.

The transport and trajectories of the particulate matter with an aerodynamic diameter less or equal than 2.5 μm ($PM_{2.5}$) were modeled with the HYSPLIT model, user account 182 (Draxler and Hess, 1997). 118 days of the cold-dry climate months of 2018 (January 1st to January 30th, February 1st to February 28th, November 1st to November 30th, and December 1st to December 30th) were modeled hourly to analyse the $PM_{2.5}$ outgoing-incoming among the three metropolitan areas. The NCEP/NCAR Global Reanalysis Data and Global Data Assimilation System (GDAS) was used as well as data/image provided by the NOAA Physical Sciences Laboratory, Boulder, Colorado, USA, from their website at https://psl.noaa.gov/. They are high-resolution data systems (32 km × 29 pressure levels and 0.5 degrees × 24 pressure levels, respectively). Both systems allow modeling dispersion of plumes and trajectory paths with high resolution (100 m). Using those meteorological data with the Hysplit model, is possible to quantify the particulate mass in areas of 1 × 1 km and 1E-16 g/h of mass transfer through metropolitan areas; the highest resolution of meteorological data would improve the spatial resolution to less than 1 × 1 km, however, considering the mass transfer estimation, the profit would be unjustified in comparison with the 5 × 5 km resolution. HYSPLIT allows a text file generation which can be used with ArcGis and MatLab to carry out the mass estimations, whereas other models only provide images and formats which are not useful for mass calculation. The meteorology data of the NCEP/NCAR Global Reanalysis Data and Global Data Assimilation System (GDAS) were downloaded from the web page of the National Oceanic and Atmospheric Administration (NOAA, 2022).

Hysplit outputs were post-processed for mass calculation, statistical analysis, and map design with ArcMap®, MatLab R2016b®, and QGis®. A geodatabase included layers of metropolitan areas polygons, the grid of cells with a resolution of 5 × 5 km (polygons and centroids), georeferenced point and area sources of $PM_{2.5}$, and georeferenced roads. The general outline of the process is displayed in Fig. 2.

The particle mass was calculated applying Eq. 1.

$$m = \sum C_i * A_i * H \quad (1)$$

Where, by every polygon: *i*, m is the mass of $PM_{2.5}$ in grams [g] dispersed inside one.

metropolitan area. Ci is the $PM_{2.5}$ concentration in grams per cubic meter [g m^{-3}]. *Ai* is the area of the polygon with concentration *Ci* in square meters [m^2].

By making geographic intersections between the hourly concentration polygons and the metropolitan areas polygons, it was possible to count the number of hours in which particles emitted in a metropolitan area crossed the borders of another metropolitan area.

Due to the particles dispersion a concentration gradient forms in three dimensions, Hysplit reports the vertical average of a column of height *H* in meters [m]. In order to quantify all the modeled particles within the spatial domain, H was calculated up to the modeled vertical top height, 2000 m.

Forward trajectories were modeled considering the planetary boundary layer with a top height of 2000 m above ground level; the planetary boundary layer also encompasses part of the mixed layer. The setup file of Hysplit was configured to consider 2500 particles released per cycle and 1E9 as the maximum number of particles. The emissions height of point and area sources were modeled to ten meters and mobile emissions to zero meters (ground level).

New clustering spatial analysis techniques developed in geographic information systems allow us to make additional interpretations to those available in Hysplit. The direction of trajectories is indeed important to identify the directional trends and potentially

Table 2
$PM_{2.5}$ mass retention statistics in the dry-cold climate months in 2018.

Statistics	TVMA				MCMA				CMA			
	Jan	Feb	Nov	Dec	Jan	Feb	Nov	Dec	Jan	Feb	Nov	Dec
Mean [kg]	272	343	353	332	1616	2556	2283	2209	96	138	132	110
Std dev. [kg]	172	305	267	261	1028	1551	1436	1461	68	140	130	89
Coeff. of variation	0.63	0.89	0.76	0.79	0.6	0.6	0.6	0.7	0.71	1.02	0.98	0.81
Minimum [kg]	19	38	38	37	169	154	161	158	11	11	12	12
Maximum [kg]	1201	1600	1579	1476	6101	7052	6710	7032	507	842	850	598
Range [kg]	1182	1562	1540	1438	5932	6898	6549	6874	496	831	838	587
Bias (std)	16.5	17.2	15.4	14.5	12.3	5.5	6.2	9.8	33.3	28.5	27.9	29.8
Kurtosis (std)	16.7	12.6	11.1	7.4	7.3	−3.0	−2.7	1.3	56.8	40.0	39.0	45.2

impacted areas with wide knowledge. The trajectories directional distribution is a more complete clustering analysis. The trajectories distribution is statistically analyzed by estimating the standard deviation of coordinates X and Y and is more clearly represented by an elliptic form. Additionally, the linear directional mean calculation is a global representation of overall trajectories. Directional distribution and lineal directional mean of trajectories were calculated to identify the most impacted areas by the pollutant transport and monthly trends of modeled trajectories.

Directional distribution and lineal directional mean of trajectories were calculated to identify the most impacted areas and trends of pollutant transport (ESRI, 2022a, 2022b). The directional distribution of trajectories was identified by the standard deviational ellipses estimated, given as:

$$C = \begin{pmatrix} \mathrm{var}(x) & \mathrm{cov}(x,y) \\ \mathrm{cov}(y,x) & \mathrm{var}(y) \end{pmatrix} = \frac{1}{n}\begin{pmatrix} \sum_{i=1}^{n}\tilde{X}_i^2 & \sum_{i=1}^{n}\tilde{x}_i\tilde{y}_i \\ \sum_{i=1}^{n}\tilde{x}_i\tilde{y}_i & \sum_{i=1}^{n}\tilde{y}_i^2 \end{pmatrix} \quad (2)$$

Where:

$$\mathrm{var}(x) = \frac{1}{n}\sum_{i=1}^{n}(x_i - \bar{x})^2 = \frac{1}{n}\sum_{i=1}^{n}\tilde{x}_i^2 \quad (3)$$

$$\mathrm{var}(y) = \frac{1}{n}\sum_{i=1}^{n}(y_i - \bar{y})^2 = \frac{1}{n}\sum_{i=1}^{n}\tilde{y}_i^2 \quad (4)$$

$$\mathrm{cov}(x,y) = \frac{1}{n}\sum_{i=1}^{n}(x_i - \bar{x})(y_i - \bar{y}) = \frac{1}{n}\sum_{i=1}^{n}\tilde{x}_i\tilde{y}_i \quad (5)$$

Where x and y are the coordinates for feature I; $\{\bar{x}, \bar{y}\}$ represent the mean center for the features and n is equal to the total number of features. C is the covariance matrix solved in ArcMap and n is equal to the total number of features.

The linear directional mean (LDM) was calculated as:

$$LDM = \arctan\frac{\sum_{i=1}^{n}\sin\theta_i}{\sum_{i=1}^{n}\cos\theta_i} \quad (6)$$

Where θ_i are the directions of one polyline feature set from a single origin.

3. Results and discussion

The methodology implemented in this study made it possible to estimate the PM2.5 mass exchange among metropolitan areas during dry-cold climate months. For the study area was possible to estimate quantities exchanged in high resolution, as small as 0.136 g/ h, and as large as 3046 kg/ h. Quantifying the exchange is available to analyse the relevance of the dynamic transport of pollutants among urban areas. Some limitation of this work is that contributions of secondary $PM_{2.5}$ and those due to the biomass burning were not included, because the necessary information to do it is not available in the emission inventory; nevertheless, the study could be done in further researchers considering data from specific studies or new information that could be generated.

The mass exchange has a cyclic behavior, associated to both meteorological variables (combined or individualized): the wind direction and the dial temperature. Generally, the dial temperature expands the mixed layer and facilitates the overflow of winds over mountainous regions. However, strong winds could force the natural advection through different orographic channels. The hourly emissions modeled in the studied metropolitan areas were 203.8 kg/ h in TVMA, 860.6 kg/ h in the MCMA, and 114.2 kg/ h in the CMA. $PM_{2.5}$ emitted in TVMA were present in 90% and 54% of the modeled hours in the MCMA and CMA, respectively; while particles emitted in MCMA were present in the TVMA and CMA, 89% and 70% of hours, respectively. The CMA exports with a lower frequency to TVMA and MCMA; just 27% of the hours, the mass of primary particles emitted in the CMA were present in the TVMA, and

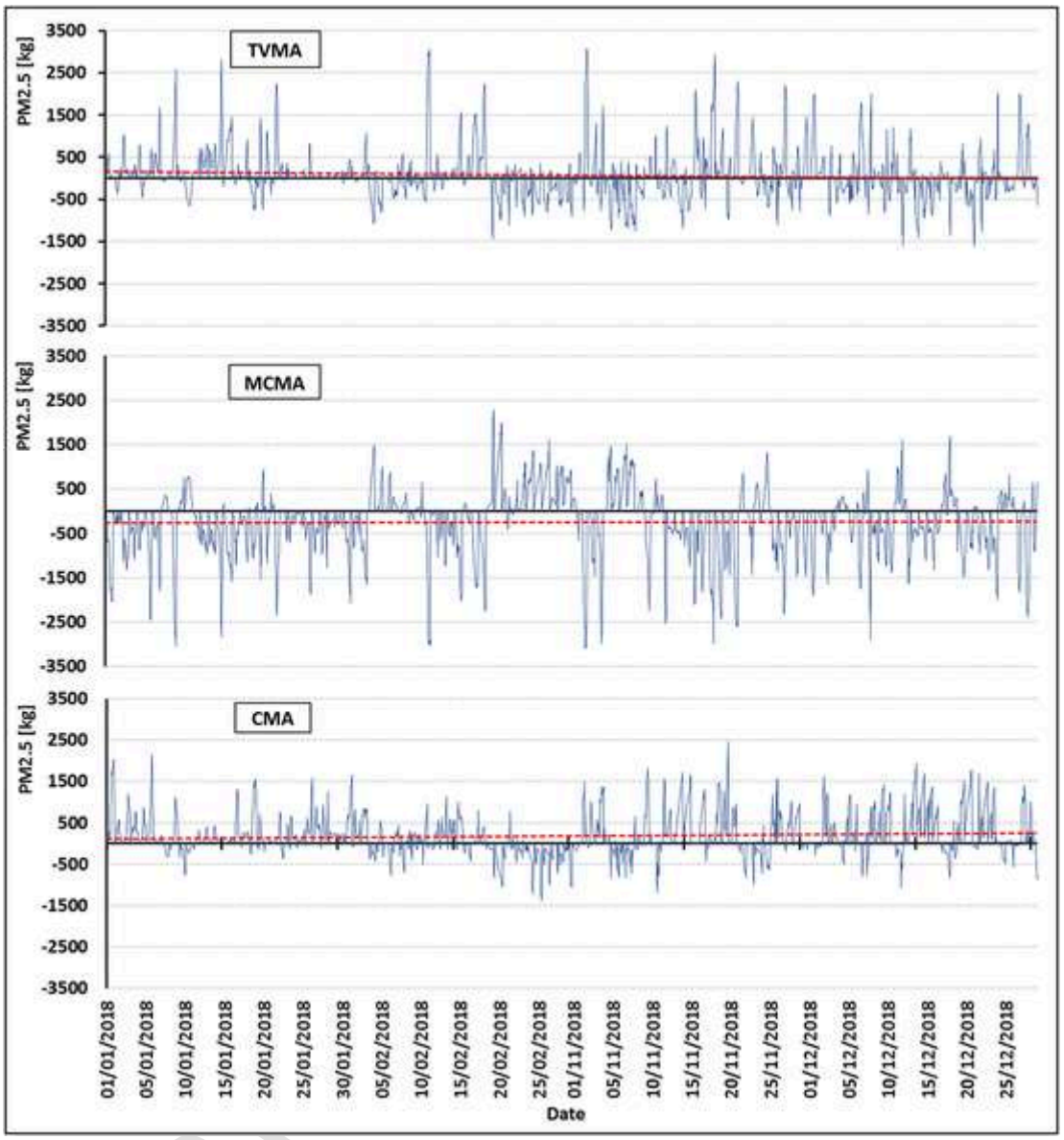

Fig. 6. Hourly mass exchange balance by metropolitan area. The blue line is the hourly balance. The red broken line is the trend line. When the trend line is above zero, the metropolitan area mass importations are greater. When the trend line is below zero, the metropolitan area mass exports are greater than the imports. UTC Time. (For interpretation of the references to colour in this figure legend, the reader is referred to the web version of this article.)

48% of the hours in the MCMA. The CMA emissions were dispersed to the southern region of Mexico mainly. Fig. 3 is a disaggregated description of these frequencies.

The most impacted areas were identified and displayed in Fig. 4. The dispersion trajectories of emissions from TVMA impacted with high frequency the Mexico State southwest and the Balsas river depression. The emissions of TVMA impacted the CMA in February, since an orographic channel between TVMA and CMA connecting the region of Xalatlaco, Mexico State, and Huitzilac, Morelos, allowed a wind flow through TVMA and CMA. The north of TVMA was impacted in December mainly. The north of the Toluca basin was unexpectedly less impacted considering that is north-northwest of the TVMA, however, the results are explained by the dominant winds from north-northeast that enter the Toluca basin. In the cold-dry months, MCMA emissions impact the east, south, and southeast zones. In general, the MCMA impacts CMA and TVMA (and other surrounding areas) in the cold-dry months. Trajectory trends are in agreement with previous wind direction reports in the MCMA in winter, frequently associated with the northerlies (Barrett and Raga, 2016; De Foy et al., 2008; García-Reynoso et al., 2009). The CMA is frequently impacted by flows driven above Tenango del Aire as was explained in previous studies (CCA-UNAM, 2016), but we identified the orographic channel close to Ozumba municipality. Although INECC (2015) identified impacts to the north of TVMA by MCMA emissions, those events were less frequent in the cold-

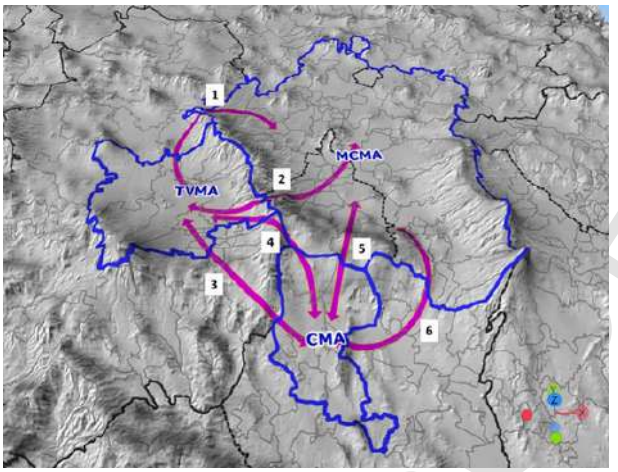

Fig. 7. Main channels of air pollutants exchange through CMA, TVMA, and MCMA. 1) Juquipilco channel. 2) Cuajimalpa channel. 3) Ocuilán channel. 4) Xalatlaco Channel. 5) Milpa Alta Channel. 6) Ozumba channel.

dry months by the MCMA emissions in 2018. The CMA trajectories were more dispersed and occasionally impacted the MCMA and TVMA, however, they frequently impacted the Morelos state southern regions as was reported by Salcedo et al. (2012).

The exchange rate of PM2.5 mass among metropolitan areas was quantified. The results indicate that TVMA and CMA bring in more mass of pollutants compared with their outward emissions. Instead, the MCMA exports more pollutant mass than its incoming flow. The TVMA can send out up to 1772.3 kg hr^{-1} of primary PM2.5 to MCMA (20/02/2018 22:00 UTC) and 1834.9 kg hr^{-1} to CMA (15/12/2018 23:00 UTC). The MCMA exports up to 2162.1 kg hr^{-1} of primary PM2.5 to CMA (06/01/2018 17:00 UTC) and 3046 kg hr^{-1} to TVMA (11/02/2018 23:00 UTC). Likewise, the CMA exported just a mass of 987.9 kg hr^{-1} to MCMA (24/11/2018 23:00 UTC) and 919.5 kg hr^{-1} to TVMA (12/11/2018 17:00 UTC). Figs. S1, S2, and S3 in Supplementary Material display the hourly profiles of PM2.5 mass emissions and incomings by each metropolitan area.

A fraction of generated emissions in a metropolitan area is temporarily kept inside the atmospheric basin. The quantification of the mass retention was graphed in Fig. 5 to analyse monthly trends of mass retention in each metropolitan area. Seasonal meteorology defines the ventilation efficiency, but even if the air dynamics is, by definition, native to the atmospheric basin, a similar effect had been observed in the quantified metropolitan areas. The mass present in one hour in the TVMA had a retention of 272 kg that represents 25% more than local hourly emissions on average, indicating bad ventilation. The standard deviation was 172 kg, thus meaning that some days the mass of PM2.5 is retained and accumulated until achieving three times the local emissions. January was the month with less PM2.5 retention in all metropolitan areas, while February and November were the months with more retention noticed. Although the CMA generated less mass of PM2.5, and the ventilation was good, the peaks of mass retention were more pronounced and frequent than TVMA and MCMA cases (note outliers). Table S1 summarizes the incomings and outgoings through the studied metropolitan areas.

In the TVMA, January was the cold-dry month with less retention, as well as less pronounced peaks (mean = 272 kg, std. dev = 172 kg). November was the month with more retention of local emissions. Consequently, it displayed higher frequency of peaks (mean = 353 kg, std. dev. = 267 kg). A comparison of outliers is shown in the box plots of Fig. 5, which represent the mass retention peaks. Also, it means that homogeneity of mass retention (width of the box) is comparable. Similar behavior was observed in January for the CMA and MCMA, which evidences the hemispheric predominant meteorology in the center of Mexico. Northern winds remove important quantities of $PM_{2.5}$ mass from TVMA and MCMA in January. The month with more retention of local MCMA emissions was February. The retention of local emissions causes higher export emissions than fresh hourly emissions, because the pollutant mass is accumulated inside the exporter basin.

Even when local emissions are lower and natural ventilation is good, when mass retention occurs, the peaks are much more pronounced concerning mean retention (variation coefficient = 101.77%). Particulate matter retention from local emissions is fairly homogeneous (Table 2), so ambient $PM_{2.5}$ concentrations would be expected to be more constant.

The MCMA is the most benefited by exchange dynamics. The mass that MCMA exports per hour could reach quantities like the daily emissions. In the exchange balance, the MCMA had a net benefit in the cold-dry season in 2018. The broken red line in Fig. 6 displays the temporal profile of the exchange balance. The trend line in the TVMA and CMA keeps above zero, demonstrating that on average, the incomings in those metropolitan areas are bigger than outgoings. On the contrary, in the MCMA the trend line keeps under zero during cold-dry months in 2018. Sometimes, the incoming fluxes are larger than the local emissions produced by CMA and TVMA. This means that, sometimes, the CMA and TVMA air quality is defined by imported emissions.

Six wind channels were identified by the trajectories modeling during the cold-dry months (Fig. 7). The orographic channels are the main routes for superficial winds to exchange pollutants, since the surface winds are channelled close to the ground by mountains until reaching the orographic channels. The identified channels were named after the municipality near the confluent trajectories among metropolitan areas or atmospheric basins. The channels 2, 3, 5, and 6 in Fig. 7 were previously identified by other authors like

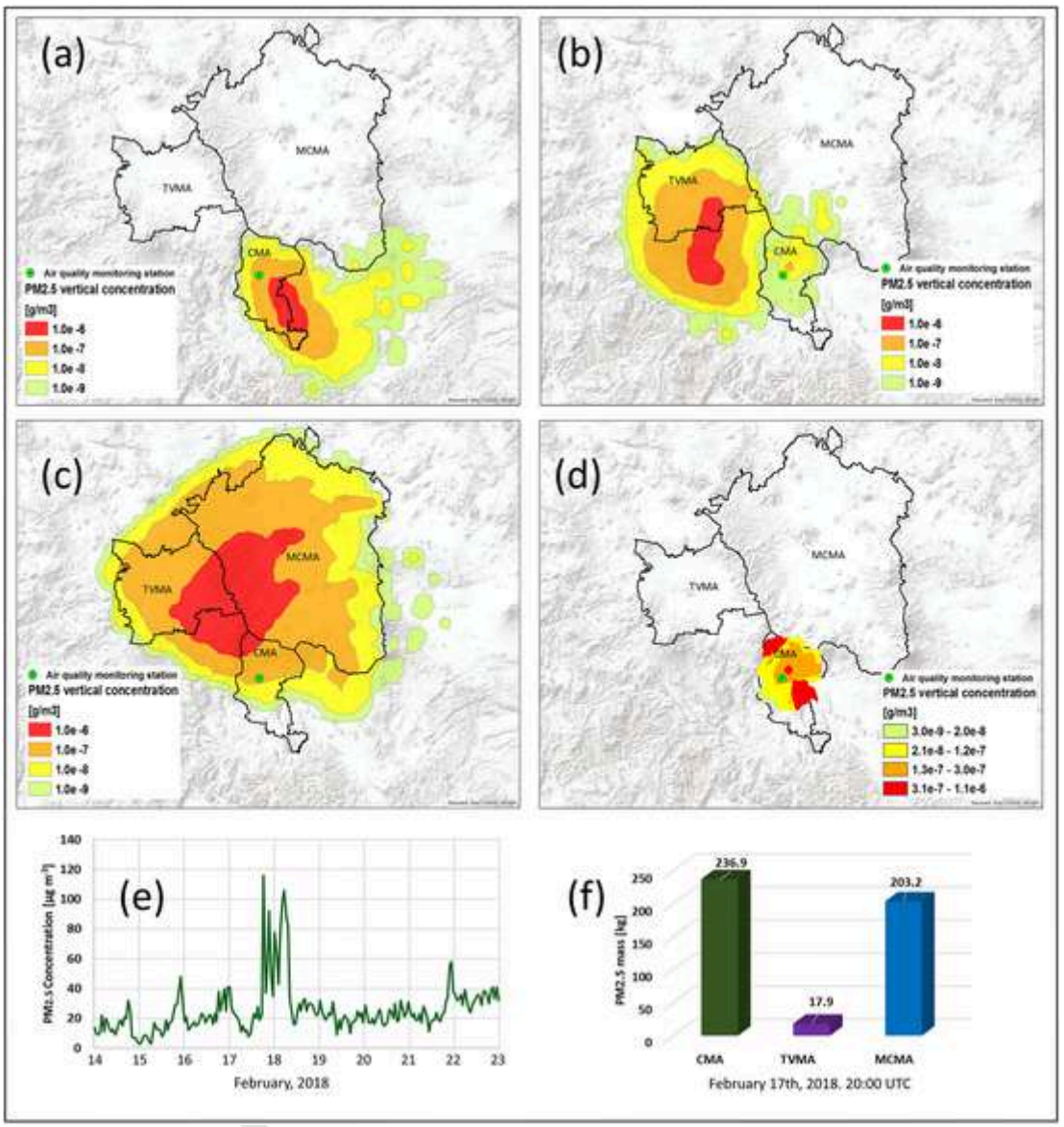

Fig. 8. Overlapping puffs of $PM_{2.5}$ over the CMA on February 17th, 2018 at 20:00 UTC. (a) Dispersion of CMA $PM_{2.5}$ emissions. (b) Dispersion of TVMA $PM_{2.5}$ emissions. (c) Dispersion of MCMA $PM_{2.5}$ emissions. (d) The addition of three overlapped puffs. (e) SINAICA data of $PM_{2.5}$ concentrations in the Cuernavaca air quality monitoring station. (f) Origin of $PM_{2.5}$ mass present on CMA on February 17th, 2018 at 20:00 UTC.

De Foy et al. (2008). Additionally, channel 1 allows bidirectional flows between the northwest of MCMA and the north of TVMA nearby Juquipilco, Mexico State. Winds from the Tula atmospheric basin sweep along the mass arriving from west of MCMA to drop in the TVMA, and vice versa. Channel 4 crosses the Neovolcanic mountain range to exchange winds between CMA and TVMA until the main flows of pollutants exported from TVMA settle to the south of México State and north of Guerrero state.

Particles emitted in one metropolitan area cross to other areas magnifying the local concentrations. Modeling separately the dispersion for each metropolitan area was possible to identify these movements and quantify the PM2.5 mass export throughout one day. The puffs could overlap in any region, but frequently this process takes place in an urban area. The sum of pollutant masses increases the PM2.5 concentrations, thereby exposing the population as result of the imports. Fig. 8 displays one example of that overlapping process where the emissions of TVMA and MCMA are overlapped above the CMA. On February 17th, 2018 an atypical increase in $PM_{2.5}$ concentrations was reported by the air quality station and no explanation was found for this high pollution event. According with the results of this research, the suggestion is that the $PM_{2.5}$ mass present in the CMA was 93% higher than local emissions by imports of TVMA and MCMA pollutant mass and puffs overlapping. These results show that the present methodology for mass exchange analysis can contribute to the explanation of high pollution events, as well as encourage the design of regional public policies considering the pollutants mass exchanges among several cities, to be included in the local and/or regional programs to improve air quality.

4. Conclusions

The primary pollutants transport emitted from the MCMA to neighboring metropolitan areas has been reported in previous studies, however, the $PM_{2.5}$ imports and exports among the metropolitan areas of Toluca Valley, Cuernavaca, and Mexico City in the cold-dry months were modeled and quantified for the first time. Results demonstrated that the MCMA impacts neighboring areas with significant quantities of pollutant masses. In the import-export balance, the CMA and TVMA have a surplus of $PM_{2.5}$ mass, whereas, the MCMA exports more pollutant mass than its imports. In one day, the $PM_{2.5}$ incomings of TVMA and CMA could be as large as local emissions, or higher. The pollutant transport trajectories in the cold-dry months had a directional distribution that mainly impacts the southern region. The TVMA exports trajectories impacted the southern of Mexico State; the Cuernavaca exports impacted the southern of Morelos State, and the MCMA mass trajectories impacted both, TVMA and CMA significantly.

When air quality monitoring authorities report unhealthy conditions, usually those situations motivate more local environmental management programs, however, if the masses of pollutant incomings are taken into account, this will allow to reconsider the pertinence and relevance of regional programs. The study of $PM_{2.5}$ emissions exchange in other seasons is necessary to have the whole scenario and a better understanding of atmospheric pollution in the Megalopolis.

Authors statement

During the preparation of this work the authors have not used generative AI and AI-assisted technologies in the writing process of this manuscript.

Uncited references

Declaration of Competing Interest

Authors declare that there is no conflict of interest, financial or other.

Data availability

Data will be made available on request.

Acknowledgements

The author would like to thank to the National Humanities, Science and Technology Council (Conahcyt) for project 316642 funding. Authors thank also to the General Management Direction of Air Quality and Pollutant Emissions and Transference Register of the Environment and Natural Resources Ministry (SEMARNAT, by the Spanish Acronym) by sharing the last Megalopolis Emission Inventory.

Appendix A. Supplementary data

Supplementary data to this article can be found online at https://doi.org/10.1016/j.uclim.2023.101608.

References

Badia, A., Vidal, V., Ventura, S., Curcoll, R., Segura, R., Villalba, G., 2023. Modeling the Impacts of Emission Changes on O 3 Sensitivity, Atmospheric Oxidation Capacity and Pollution Transport Over the Catalonia Region. x. pp. 1–38.

Balakrishnan, K., Brauer, M., Chen, G., Chow, J., 2015. Outdoor air pollution. In: IARC monographs (Vol. 109). International Agency for Research on Cancer. https://publications.iarc.fr/538.

Barrett, B.S., Raga, G.B., 2016. Variability of winter and summer surface ozone in Mexico City on the intraseasonal timescale. Atmos. Chem. Phys. 16 (23), 15359–15370. https://doi.org/10.5194/ACP-16-15359-2016.

Bera, B., Bhattacharjee, S., Sengupta, N., Saha, S., 2022. Variation and dispersal of PM10 and PM2. 5 during COVID-19 lockdown over Kolkata metropolitan city, India investigated through HYSPLIT model. Geosci. Front. 13 (1), 101291.

CAMe, 2018. Comisión Ambienal de la Megalópolis. Progr. Gest. Fede. Para Mejorar Calidad Aire Megalópolis 2017–2030.

CCA-UNAM, 2016. Diagnóstico sobre la calidad del aire en cuencas atmosféricas de México.

Chacón, D., Palacios, R., Correa, C., Chavana, M., 2021. Estudio sobre la influencia de la central termoeléctrica de Tula, Hidalgo, en la calidad del aire regional. https://www.iniciativaclimatica.org/wp-content/uploads/2021/05/Termoeléctrica-Tula_190521-3-1.pdf.

De Foy, B., Varela, J.R., Molina, L.T., Molina, M.J., 2006. Rapid ventilation of the Mexico City basin and regional fate of the urban plume. Atmos. Chem. Phys. 6 (8), 2321–2335. https://doi.org/10.5194/acp-6-2321-2006.

De Foy, B., Fast, J.D., Paech, S.J., Phillips, D., Walters, J.T., Coulter, R.L., Martin, T.J., Pekour, M.S., Shaw, W.J., Kastendeuch, P.P., Marley, N.A., Retama, A., Molina, L.T., 2008. Basin-scale wind transport during the MILAGRO field campaign and comparison to climatology using cluster analysis. Atmos. Chem. Phys. 8 (5), 1209–1224. https://doi.org/10.5194/acp-8-1209-2008.

Dedoussi, I.C., Eastham, S.D., Monier, E., Barrett, S.R.H., 2020. Premature mortality related to United States cross-state air pollution. Nature 578 (7794), 261–265. https://doi.org/10.1038/s41586-020-1983-8.

DOF, 2013. Convenio de Coordinación por el que se crea la Comisión Ambiental de la Megalópolis, que celebran la Secretaría de Medio Ambiente y Recursos Naturales, el Gobierno del Distrito Federal y los estados de Hidalgo, México, Morelos, Puebla y Tlaxcala. Diario Oficial de La Federación. pp. 1–7. https://www.gob.mx/cms/uploads/attachment/file/332496/CONVENIO_CREACIO_N_CAME_DOF.pdf.

Draxler, R.R., Hess, G.D., 1997. Description of the HYSPLIT_4 modeling system. In: NOAA Tech. Memo. ERL ARL-224. NOAA Air Resources Laboratory. https://

www.arl.noaa.gov/wp_arl/wp-content/uploads/documents/reports/arl-224.pdf.
Emmons, L.K., Apel, E.C., Lamarque, J.-F., Hess, P.G., Avery, M., Blake, D., Brune, W., Campos, T., Crawford, J., DeCarlo, P.F., Hall, S., Heikes, B., Holloway, J., Jimenez, J.L., Knapp, D.J., Kok, G., Mena-Carrasco, M., Olson, J., O'Sullivan, D., Wiedinmyer, C., 2010. Impact of Mexico City emissions on regional air quality from MOZART-4 simulations. Atmos. Chem. Phys. 10 (6195–6212), 2010. https://doi.org/10.5194/acp-10-6195-2010.
ESRI, 2022a. How Directional Distribution (Standard Deviational Ellipse) Works. https://resources.arcgis.com/en/help/main/10.2/index.html#//005p0000001q000000.
ESRI, 2022b. How Linear Directional Mean works. https://desktop.arcgis.com/en/arcmap/latest/tools/spatial-statistics-toolbox/h-how-linear-directional-mean-spatial-statistics-w.htm.
Flores-Ortiz, A., Jiménez-Núñez, M. da le L., Venancio, R., Godoy, D., 2021. Study of the behavior of air parcels, using PIXE, Hysplit and wind rose in the metropolitan zone of Toluca Valley, Mexico. J. Energy Res. Rev. 9 (1), 51–66. https://doi.org/10.9734/JENRR/2021/v9i130225.
García-R, A., Schoenemeyer, T., Jazcilevich, A., Ruíz-Suárez, G., Fuentes-Gea, V., 2000. Implementation of the multiscale climate chemistry model (MCCM) for Central Mexico. In: H. P, J. W. L, Brebbia, C.A. (Eds.), Air Pollution, vol. VIII. WIT Press.
García-Reynoso, A., Ruiz-Suárez, L.G., García-Escalante, J.S., Reséndiz-Juárez, N., 2009. Comportamiento de los contaminantes en cuencas atmosféricas: metodología y estudio de caso.
González, M.C., Cerezo, A., González, M.D.C., Salazar, L., 1999. Comportamiento de las partículas suspendidas y polen en la atmósfera de la región norte de la Zona Metropolitana de la Ciudad de México. J. Mex. Chem. Soc. 43 (5), 155–164.
González-Cardoso, G., Hernández-Contreras, J., Valle-Hernández, B., Hernández-Moreno, A., Santiago-De la Rosa, N., García-Martínez, R., Mugica-Álvarez, V., 2020. Toxic atmospheric pollutants from crematoria ovens: characterization, emission factors, and modeling. Environ. Sci. Pollut. Res. 27, 43800–43812.
Hoek, G., Krishnan, R.M., Beelen, R., Peters, A., Ostro, B., Brunekreef, B., Kaufman, J.D., 2013. Long-term air pollution exposure and cardio- respiratory mortality: a review. Environ. Health 12 (43), 1–15. . https://ehjournal.biomedcentral.com/articles/10.1186/1476-069X-12-43.
Huang, R., Qin, M., Hu, Y., Russell, A.G., Odman, M.T., 2020. Apportioning prescribed fire impacts on PM2. 5 among individual fires through dispersion modeling. Atmos. Environ. 223, 117260.
IARC, 2016. IARC monographs on the evaluation of carcinogenic risks to humans: Outdoor air pollution. In: IARC monographs, vol. 109. World Health Organization. https://monographs.iarc.who.int/.
INECC, 2015. Estudios de Calidad del Aire y su Impacto en la Región Centro de México. Centro de Ciencias de la Atmósfera.
Jazcilevich, A.D., García, A.R., Ruíz-Suárez, L.G., 2003. A study of air flow patterns affecting pollutant concentrations in the central region of Mexico. Atmos. Environ. 37 (2), 183–193. https://doi.org/10.1016/S1352-2310(02)00893-2.
Magaña, V., Caetano, E., 2007. Identificación de Cuencas Atmosféricas en México.
Molina, L.T., Velasco, E., Retama, A., Zavala, M., 2019. Experience from integrated air quality management in the Mexico City metropolitan area and Singapore. Atmosphere 10 (9), 512.
NOAA, 2022. Air resources laboratory. HYSPLIT. https://www.ready.noaa.gov/HYSPLIT.php.
Ortinez-Alvarez, A., Ruiz-Suarez, L.G., Ortega, E., Garcia-Reynoso, A., Peralta, O., Lopez-Gaona, A., Castro, T., Martinez-Arroyo, A., 2021. Emission inventory point source visualization on Google Earth and integrated with HYSPLIT model *(edited by Dr. Luisa Molina)*. Atmósfera 34 (2), 143–156. https://doi.org/10.20937/ATM.52834.
Salcedo, D., Castro, T., Ruiz-Suárez, L.G., García-Reynoso, A., Torres-Jardón, R., Torres-Jaramillo, A., Mar-Morales, B.E., Salcido, A., Celada, A.T., Carreón-Sierra, S., Martínez, A.P., Fentanes-Arriaga, O.A., Deustúa, E., Ramos-Villegas, R., Retama-Hernández, A., Saavedra, M.I., Suárez-Lastra, M., 2012. Study of the regional air quality south of Mexico City (Morelos state). Sci. Total Environ. 414, 417–432. https://doi.org/10.1016/J.SCITOTENV.2011.09.041.
SEMARNAT, 2016. Elementos para inventarios de fuentes móviles. In: Informe Final 2016, 52, Issue 55. Secretaría de Medio Ambiente y Recursos Naturales.
SEMARNAT, 2022. Inventario de Emisiones de la Megalópolis 2018. Secretaría de Medio Ambiente y Recursos Naturales. Provided by the corresponding authorities, since it is not yet a public document.
Sergi, B., Azevedo, I., Davis, S.J., Muller, N.Z., 2020. Regional and county flows of particulate matter damage in the US. Environ. Res. Lett. 15 (10), 104073. https://doi.org/10.1088/1748-9326/ABB429.
Sisneros, M., 2014. Evaluation Of Ozone Trends In Southern Doña Ana County, New Mexico Thru Wind Rose Analysis And Use Of NOAA HYSPLIT Model. Open Access Theses & Dissertations. https://scholarworks.utep.edu/open_etd/1737.
SMAEM, 2007. Cuencas atmosféricas del Estado de México. Gobierno del Estado de México. https://sma.edomex.gob.mx/sites/sma.edomex.gob.mx/files/files/sma_pdf_2007_ca_em.pdf.
Tran, T., Kumar, N., Knipping, E., 2023. Investigating sensitivity of ozone to emission reductions in the new York City (NYC) metropolitan and downwind areas. Atmos. Environ. 301 (February), 119675. https://doi.org/10.1016/j.atmosenv.2023.119675.
Tzompa-Sosa, Z.A., Sullivan, A.P., Retama, A., Kreidenweis, S.M., 2016. Contribution of biomass burning to carbonaceous aerosols in Mexico City during may 2013. Aerosol Air Qual. Res. 16 (1), 114–124.
Yerramilli, A., Dodla, V.B.R., Challa, V.S., Myles, L., Pendergrass, W.R., Vogel, C.A., Dasari, H.P., Tuluri, F., Baham, J., Hugues, R., Patrick, Ch., Young, J.H., Swanier, S., Hardy, M.G., 2012. An integrated WRF/HYSPLIT modeling approach for the assessment of PM2. 5 source regions over the Mississippi Gulf Coast region. Air Qual. Atmos. Health 5 (4), 401–412.